FEBRUARY 1975   MATT-1113

FAST-WAVE HEATING OF A
TWO-COMPONENT PLASMA

BY

THOMAS H. STIX

PLASMA PHYSICS
LABORATORY

MASTER

PRINCETON   UNIVERSITY
PRINCETON, NEW JERSEY

DISCLAIMER

This report was prepared as an account of work sponsored by an agency of the United States Government. Neither the United States Government nor any agency Thereof, nor any of their employees, makes any warranty, express or implied, or assumes any legal liability or responsibility for the accuracy, completeness, or usefulness of any information, apparatus, product, or process disclosed, or represents that its use would not infringe privately owned rights. Reference herein to any specific commercial product, process, or service by trade name, trademark, manufacturer, or otherwise does not necessarily constitute or imply its endorsement, recommendation, or favoring by the United States Government or any agency thereof. The views and opinions of authors expressed herein do not necessarily state or reflect those of the United States Government or any agency thereof.

DISCLAIMER

Portions of this document may be illegible in electronic image products. Images are produced from the best available original document.

Fast-Wave Heating of a Two-Component Plasma[*]

THOMAS H. STIX

Plasma Physics Laboratory, Princeton University

Princeton, New Jersey 08540 USA

ABSTRACT

The use of the compressional hydromagnetic mode
(also called the magnetosonic or, simply, the fast wave)
is examined in some detail with respect to the heating
of a tritium plasma containing a few percent deuterium.
Efficient absorption of wave energy by the deuteron
component is found when $\omega = \omega_c$ (deuterons), with
$Q_{wave} \gtrsim 100$. Reasonable efficiencies are found also for
electron heating, but coherence effects between transit-
time and Landau damping for electrons reduce the total
absorption for both processes to one-half of the transit-
time power, calculated separately.

The fusion output of a two-component neutral-
injected plasma can be enhanced by selective heating of
the injected deuterons. Also, selective deuteron
absorption may be used for ion-tail creation by radio-
frequency excitation <u>alone</u>, as an alternative to neutral
injection. The dominant behavior of the high-energy
deuteron distribution function is found to be
$f(v) \sim \exp[(3/2)\int^V dv <\Delta v>/<(\Delta v_\perp)^2>]$, where $<\Delta v>$ is the
Chandrasekhar-Spitzer drag coefficient, and $<(\Delta v_\perp)^2>$ is
the Kennel-Englemann quasilinear diffusion coefficient

for wave-particle interaction at the deuteron cyclotron frequency. An analytic solution to the one-dimensional Fokker-Planck equation, with rf-induced diffusion, is developed, and using this solution together with Duane's fit to the D-T fusion cross-section, it is found that the nuclear fusion power output from an rf-produced two-component plasma can significantly _exceed_ the incremental (radiofrequency) power input.

1. INTRODUCTION

The need for supplementary heating for a tokamak — supplementary, that is, to the Ohmic heating associated with the toroidal current — has been recognized for a number of years. Only recently, however, have the special benefits become clear for a specific form of supplementary heating: putting the heat in as a high-energy tail on the ion distribution. In bringing a classical (50-50) DT reactor to ignition, the high energy ions cause fusion reactions which release alpha particles and enhance the heating power, while in the two-component fusion device [1], the creation of the ion tail is an essential element of the total concept.

The most direct way to produce the ion tail is evidently by neutral injection. It will be some years, however, before neutral beam technology allows us to test this heating method at the requisite beam currents and voltages, and the final answers on efficiency, penetration, impurities, plasma stability, and beam slowdown rates must await such testing. Meanwhile, it is appropriate to look at radiofrequency methods as an alternative process for plasma heating and for ion tail creation. Radiofrequency heating can play a number of roles:

a. Electron heating. A successful two-component fusion experiment needs an electron temperature of 5 keV or more. Neutral injection provides supplementary heat to both the background ions and electrons, and too much background ion heating can be wasteful. In addition, it may turn out that rf electron heating is less costly to install than injection heating with similar capability.

b. Supplementary heating. Supplementary ion heating is the traditional role assigned to rf heating.

c. Ion tail creation. Selective absorption of rf energy by a minority of the plasma ions may be achieved by cyclotron resonance tuned to the minority ions [2-4], or by cyclotron harmonic heating which preferentially delivers power to the high energy (large Larmor radius) component [4-6].

d. Ion tail enhancement. Radiofrequency heating may be used to enhance neutral injection itself by tuning the rf to resonance with the injected beam particles in the plasma. Such heating can easily add perpendicular energy to beam ions, and can increase and maintain the energy dispersion of the beam and the fusion reaction rate.

The wave mode which is uncannily well suited to the various objectives outlined above is the compressional hydromagnetic wave, also called the magnetosonic mode or simply the fast wave. The wave lengths in the desired frequency ($\omega \sim \omega_{ci}$) and density ($n \sim 10^{14}$ cm^{-3}) ranges are long enough to allow reasonable mode separation in the large tokamak plasmas and good coupling to the antenna structures. Fast wave heating [7] for large plasma devices was first seriously examined by Adam and Samain[4] . On the experimental side, experiments in 1967 on the Model C-stellarator showed both fast-wave generation and plasma heating [8]. More recently, the 1974 ST tokamak experiments [9] strongly confirmed fast wave heating and, equally important, demonstrated the existence of and showed the ability to excite high-Q discrete fast-wave toroidal modes [5].

By proper selection of the fast-wave frequency, mode numbers,

magnetic field strength and plasma composition, it is possible to heat ions and/or electrons, to vary the deposition pattern of the heating, and to modify the ion velocity distribution. Using fast-wave heating equipment, the experimentalist therefore has available to him, with rather modest parameter changes, a great flexibility in his experimental approach and a great range of physical processes.

In this paper we examine in some detail the specific use of fast-wave excitation for heating large magnetically-confined toroidal plasmas. We look at electron heating through wave-absorption via Landau and transit-time damping (the two effects are coherent and cross-terms must be considered), and ion heating through cyclotron damping. A Fokker-Planck calculation with a quasilinear-type rf diffusion coefficient shows that selective rf cyclotron absorption is competitive with neutral injection for the formation of a fusion-producing two-component ion velocity distribution.

2. ALLOWED MODES AND MODE-TRACKING

We start our detailed consideration of fast-wave heating by looking at the properties of this mode in a homogeneous cold plasma immersed in a uniform static magnetic field. The wave equation can be written in the usual matrix form, with k_y set equal to zero,

$$\begin{pmatrix} K_{xx} - n_z^2 & K_{xy} & n_x n_z \\ K_{yx} & K_{yy} - n^2 & 0 \\ n_z n_x & 0 & K_{zz} - n_x^2 \end{pmatrix} \begin{pmatrix} E_x \\ E_y \\ E_z \end{pmatrix} = 0 \quad . \quad (1)$$

$n_x \equiv k_x c/\omega$ and $n_z \equiv k_z c/\omega$ are the two remaining components of the vector refractive index, $n^2 = n_x^2 + n_z^2$, and we have neglected components of the dielectric tensor, $\vec{K}$, which are finite only for $T \neq 0$. The usual low-frequency high-conductivity approximation is now taken, $|K_{zz}| >> n_x^2$, n_{xz}, and we may further denote $K_{xx} \simeq K_{yy} = S = (1/2)(R + L)$ and $K_{xy} = -K_{yx} = -iD = -(i/2)(R - L)$, leaving

$$\frac{1}{4} \begin{pmatrix} R+L-2n_z^2 & -i(R-L) \\ i(R-L) & R+L-2n^2 \end{pmatrix} \begin{pmatrix} E_x \\ E_y \end{pmatrix} \simeq 0 . \qquad (2)$$

For $|\omega| << \omega_{ce}$, ω_{pe} and neglecting displacement current, but including the electron contribution, the cold-plasma dielectric tensor elements are $R \simeq (4\pi n_i m_i c^2/B^2)[\omega_{ci}/(\omega_{ci}+\omega)]$; $L \simeq (4\pi n_i m_i c^2/B^2)[\omega_{ci}/(\omega_{ci}-\omega)]$. The dispersion relation for hydromagnetic waves is given just by the determinant of the 2×2 matrix, and may then be written

$$N_\perp^2 = A - N_\shortparallel^2 + \frac{A(1-A)}{A-N_\shortparallel^2} , \qquad (3)$$

where $N_\perp$ and $N_\shortparallel$, the Alfvén refractive indices, are defined

$$N_\perp^2 \equiv n_x^2 \left(\frac{B^2}{4\pi n_i m_i c^2} \right)$$

$$N_\shortparallel^2 \equiv n_z^2 \left(\frac{B^2}{4\pi n_i m_i c^2} \right)$$

$$A \equiv \omega_{ci}^2 / (\omega_{ci}^2 - \omega^2)$$

The dispersion relation is sketched in Fig. 1 for the two cases, $A > 1$ ($\omega < \omega_{ci}$) and $A < 0$ ($\omega > \omega_{ci}$). The curve for $\omega > \omega_{ci}$ shows the two well-known Alfvén waves, the shorter-wavelength shear or ion cyclotron mode, and the longer-wavelength compressional mode, also called the magnetosonic or fast wave. The case of especial interest to us is that where the plasma ions are predominatly tritons, but where ω is set equal to the deuteron cyclotron freqeuncy. In this case $A = -4/5$. It is instructive to draw the dispersion relation for just the propagating region of the fast wave, using $N_\perp$, $N_{||}$ as coordinates rather than $N_\perp^2$ and $N_{||}^2$, and such a plot is shown in Fig. 2. Now in a finite-geometry plasma, wavenumbers for the allowed modes will be approximate multiples of some fundamental wavenumbers, e.g., $N_{||} \simeq n N_{||}^{(0)}$, $N_\perp \simeq \nu N_\perp^{(0)}$. Therefore, the natural modes of the finite-geometry plasma will occur where the dispersion relation curve passes through an intersection of the background cartesian grid laid out with spacings corresponding to the fundamental wavenumbers, as indicated in Fig. 2. As the device size and plasma density are increased, the grid spacings in Fig. 2 will decrease. For instance, in a torus [10],

$$N_{||}^{(0)} = \frac{c}{R\omega} \left(\frac{B^2}{4\pi n_i m_i c^2} \right)^{1/2} \quad , \qquad (4)$$

$$N_\perp^{(0)} \simeq \frac{\pi c}{a\omega} \left(\frac{B^2}{4\pi n_i m_i c^2} \right)^{1/2} \quad .$$

Actually the mode spectrum is slightly more complicated than just described. The approximation that $N_\perp \simeq \nu N_\perp^{(0)}$ with $N_\perp^{(0)}$ given by Eq. 4 is valid for modes with toroidal and radial but no poloidal variation. But the complete dispersion relation for a toroidal system will have a structure similar to that given by Bernstein and Trehan [11] for a finite-radius cylinder of uniform-density cold plasma: the field amplitude varies as $B_z^{(1)} = $ constant $\cdot$ $J_m(\nu r) \exp(im\theta + ikz - i\omega t)$ and the dispersion relation is of the form

$$\frac{k_\perp a J_m'(k_\perp a)}{J_m(k_\perp a)} = A + mB$$

where A and B are functions of ω, $k_\parallel$, and the plasma parameters. Solutions of this dispersion relation appear between each pair of zeros of $J_m(k_\perp a)$ and therefore can be categorized simply by $k_\perp a \simeq \pi(r + |m/2|) + \epsilon(r,m)$, where r and m are the radial and poloidal mode numbers, and ϵ is an angle of magnitude less than π. The integer quantity we had called ν would be $\sim k_\perp a/\pi$, but we see now that the complete spectrum shows modes at half-integral values of ν, for $\nu > 1$, and each such mode has a $(2\nu - 1)$-fold multiplicity, i.e., $\nu = 1$ corresponds to $r = 1$, $m = 0$; $\nu = 3/2$ to $r = 1$, $m = \pm 1$; $\nu = 2$ to $r = 2$, $m = 0$ and $r = 1$, $m = \pm 2$, etc.

The mode spectrum for a straight cylinder is degenerate with respect to propagation parallel or antiparallel to $\hat{z}\vec{B}_o$, i.e., with respect to $\pm k_\parallel$. It has been pointed out by Chance and Perkins [12] that this degeneracy is resolved in a tokamak plasma, the line separation being related to mode rotation due to the

helical magnetic lines of force. Just as each designated ν-value in Fig. 2 is actually a $(2\nu - 1)$-fold multiplet (not shown on the drawing), it is then also true that each n value actually designates a doublet (not shown) in the spectrum. Certain important qualitative conclusions can be drawn immediately from this interpretation of Fig. 2. We consider the possibilities for fixed ω/B, corresponding to setting $\omega = \omega_{cj}$ for a j-type ion:

1. For a toroidal device which is too small in minor radius, or in which the desired density has too small a value, even the nearest grid intersection will fall outside the dispersion curve, and no natural fast-wave modes will propagate. The Princeton C-stellarator plasma fell in this category.

2. For an intermediate-size plasma, a small number of modes will be possible, and these will be reasonably well separated in density. The recent fast-wave experiments in ST fall into this category.

3. For a somewhat larger plasma, many modes will be possible, but the mode separation in density will still be large enough that rather broad-spectrum excitation can be used successfully to excite the desired single modes. Princeton's PLT, PDX, and perhaps TFTR would be in this category.

4. For reactor-size plasmas, the dense mode spectrum will tend to frustrate efforts to excite optimum single modes to achieve, say, ion heating without electron Landau damping, or core heating without surface heating. In such large devices, then, considerable attention will have to be paid to the use of antenna structures which narrow the $k_\perp$ and $k_\parallel$ excitation spectra.

5. For any plasma, the occurrence of a natural mode with specified $k_{||}$, $k_{\perp}$, ω, and B requires the proper value for ion density. In pulsed plasmas and in the start-up of steady-state plasmas, the density will vary with time, and allowance must be made for tracking resonant conditions either by varying ω or, jumping modes, by changing the $\vec{k}$-excitation spectrum.

3. $\vec{E}$-FIELD POLARIZATION

The natural sense of rotation of ions around the magnetic field lines is that of left-handed screw motion progressing along the $\vec{B}$ vector. Cyclotron acceleration of the ions therefore depends principally on the amplitude of the left-handed circularly-polarized component of the wave electric field in the plasma. In detail, if one goes to finite-Larmor-radius theory, it will be found that ion acceleration due to a pure right-hand E-field component will be weaker by a factor $\sim k_{\perp}^4 \langle \rho_{Li}^4 \rangle$ than that due to the left-hand component, a result which holds even for cyclotron-harmonic acceleration. (Examine the structure of $|\theta_{n,k}|^2$ in Eq. (18) below.) Going back to Eq. (2), we can determine the ratio of the left-hand $\vec{E}$ component $(E_x + iE_y)$ to the right-hand component $(E_x - iE_y)$,

$$\frac{E_x + iE_y}{E_x - iE_y} = -\frac{R-n_z^2}{L-n_z^2} = \frac{\dfrac{\omega_{ci}}{\omega+\omega_{ci}} - N_{||}^2}{\dfrac{\omega_{ci}}{\omega-\omega_{ci}} + N_{||}^2} \quad , \qquad (5)$$

and provided that $\omega > \omega_{ci}$ and $\omega_{ci}/(\omega + \omega_{ci}) > N_{||}^2 > 0$ (that is, for a propagating fast wave at $\omega > \omega_{ci}$), then

$$\frac{E_x + iE_y}{E_x - iE_y} < \frac{\omega - \omega_{ci}}{\omega + \omega_{ci}} \quad . \tag{6}$$

For $\omega = (3/2)\omega_{ci}$, corresponding to deuteron cyclotron resonance in a triton plasma, the right-hand side of (6) equals 1/5. The ratio in (5) is a maximum for $N_{\shortparallel}^2 = 0$ and drops to zero for parallel propagation, which is characterized by the dispersion relation $n_{\shortparallel}^2 = R$ ($n_{\perp}^2 = 0$) and pure right-hand circular polarization. (The E_L/E_R relation, Eq. (5), applies, of course, also to ion cyclotron waves, but reduction of E_L is avoided in this instance because $n_z^2 \sim L$. For dense plasmas, this condition on n_z^2 requires very short parallel wave-lengths.) The relative magnitude of the left-hand E field is also reduced if the number of resonant ions is increased — up to now, we have neglected the contribution of the resonant deuterons to the dielectric tensor. Their principal contribution is to L, but hot-plasma theory limits the magnitude even at exact resonance. Writing $L = L_T + L_D$ for the tritium (plus electrons) and deuterium components, one will find the extremum value for L_D/L_T, occurring at $\omega = \omega_{cD}$,

$$\left(\frac{L_D}{L_T}\right)^{\text{extr.}} = -\frac{i\pi^{1/2}}{3} \frac{n_D}{n_T} \frac{\omega_{cD}}{|k_z|} \left(\frac{m_D}{2kT_D^{(\shortparallel)}}\right)^{1/2} . \tag{7}$$

The power going into deuteron heating will be proportional to $n_D|E_x + iE_y|^2$ and will be a maximum for n_D such that $|L_D/L_T|^{\text{extr.}}$ is of the order of unity. Typically this leads to optimal fractional deuteron concentrations of a few percent. A similar argument

can be applied to second-harmonic heating in, for instance, a 50-50 D-T plasma. In that case, however, the contribution to L from the resonant ions is reduced by a factor proportional to $k_\perp^2 <\rho_{Li}^2>$.

4. ION CYCLOTRON DAMPING

Collisionless cyclotron damping can take place with absorption of wave energy by the particles that, in their own frame of reference, feel the wave E-field at their cyclotron frequency. The well known condition for such single-particle resonance is $\omega - k_\| v_\| = \omega_c$. We will return to the standard uniform-B calculation, but it is instructive first to calculate particle heating in the inhomogeneous tokamak magnetic field. Given ω, $k_\|$, and $v_\|$ for a test ion, resonance will occur in the neighborhood of a certain $B = $ constant surface. Ions following along the B-lines which twist around the magnetic axis can pass through the resonant surface twice each complete revolution. On each passage through resonance the ions receive a kick in $mv_\perp$ which is not difficult to calculate. The single-particle equations of motion perpendicular to $\vec{B}$ are

$$\dot{v}_x - \Omega(t) v_y = \frac{q}{m} E_x \cos\omega t$$

$$\dot{v}_y + \Omega(t) v_x = - \frac{q}{m} E_y \sin\omega t$$

Let $E_\pm \equiv (1/2)(E_x \pm E_y)$, $u \equiv v_x + iv_y$. $\Omega(t)$ is the cyclotron frequency at the instantaneous particle position. Expand $\Omega(t)$ around the resonant surface,

$$\Omega(t) = \omega + (t-t_o)\Omega'(t) + \ldots \quad .$$

The two real-variable equations can then be written as a single equation in the complex variable u,

$$\frac{du}{dt} + i\Omega(t)u = \frac{q}{m}(E_+e^{-i\omega t} + E_-e^{i\omega t}) \quad .$$

We neglect the non-resonant (E_-) driving term and integrate,

$$u(t)\exp(i\int_{-\infty}^t \Omega dt) = u(-\infty) + \frac{q}{m}E_+ \int_{-\infty}^t dt'\exp[\frac{i\Omega'(t'-t_o)^2}{2}]$$

$$\to u(-\infty) + \frac{q}{m}E_+\left(\frac{2\pi i}{\Omega'}\right)^{1/2} \quad ,$$

for $t \gg t_o$. We assume that $u(-\infty)$ is randomly phased with respect to E_+ (but will return to this point in Section 8) and compute the average change in energy per transit of the resonant surface,

$$\frac{m}{2} < u(t)u(t)^* - u(-\infty)u(-\infty)^* > = \frac{m}{2}|\frac{q}{m}E_+|^2 \cdot |\frac{2\pi}{\Omega'}| \equiv W(\vec{r}) \quad .$$

To find the total rate of power absorption per unit volume, P, we multiply the energy gained per transit, W by the total ion transiting rate, ν, forming $P = \nu(\vec{r})W(\vec{r})$. For this calculation we choose a local coordinate system in which $\hat{z}$ is the direction of the toroidal component of $\vec{B}$, $\hat{x}$ is in the direction of the major radius, and $\hat{y}$ is vertical, parallel to the major axis of the torus. The exact location of the resonant surface for each ion depends on

$v_{"}$ in order to satisfy $\omega - k_{"}v_{"} - \omega_c = 0$, and $\nu(x,y)$ is the number of ion transits across such resonant surfaces that occur per unit time in each unit volume of the plasma,

$$\left| \nu dx \right| = \int_u^{u+\Delta u} dv_z \int_{-\infty}^{\infty} dv_x \int_{-\infty}^{\infty} dv_y \left| v_{xg} \right| f(x,y,\vec{v}) \quad ,$$

where

$$u = v_{"}^{(res)} \equiv \frac{\omega - \omega_c(x)}{k_{"}} \quad ,$$

and

$$u + \Delta u = \frac{\omega - \omega_c(x+\Delta x)}{k_{"}} \quad ,$$

and where v_{xg} is the x-component of the ion guiding-center velocity. From these equations we derive

$$\Delta u = \Delta x \frac{dv_{"}^{(res)}}{dx} = - \Delta x \left(\frac{1}{k_{"}} \frac{d}{dx} \omega_{ci} \right) \quad .$$

Also, we may write

$$\Omega' = \frac{d\Omega}{dt} = \frac{d}{dt} \omega_{ci} = v_{xg} \frac{d}{dx} \omega_{ci} \quad ,$$

where v_{xg} is again the $\hat{x}$ guiding-center velocity. In forming P, it is interesting to note that v_{xg} cancels out, leading to a result which is independent of the local value of tokamak rotational transform, etc. We find simply

$$P(\vec{r}) = \frac{\pi q^2}{m|k_{"}|} \int dv_x dv_y \ f(\vec{r},\vec{v}_{\perp},v_{"}^{(res)}) |E_+(\vec{r})|^2 \qquad (8)$$

which is precisely the result one obtains [13] from conventional uniform-B hot-plasma theory. This identity of results has the

further welcome consequence that the use of the uniform-B-theory monochromatic-spectrum quasilinear diffusion coefficient may now be justified for the calculation of ion heating in the inhomogeneous B-field of a tokamak. The point will be discussed in Section 7.

The next step is to average $P(\vec{r})$ over the volume between two magnetic surfaces, of minor radii r_1 and r_2. For this purpose we write

$$f(\vec{r}, v_{\shortparallel}^{(res)}) = f[\vec{r}, \frac{\omega - \omega_{ci}}{k_{\shortparallel}}] \quad ,$$

and

$$dx = d\omega_{ci}/(d\omega_{ci}/dx) = -\frac{R}{\omega_{ci}} d\omega_{ci} \quad ,$$

and then

$$(2\pi R)\,\pi\,(r_2^2 - r_1^2) <P> = \frac{4\pi^2 q^2 R^2}{m\omega_{ci}} \int_{r_1|\sin\theta_1|}^{r_2|\sin\theta_2|} dy \; n(y)\,|E_+(y)|^2 \quad , \quad (9)$$

where $n(y)$, m and ω_{ci} refer to the resonant ions only (e.g., deuterons) and where the integral is carried out along y at a value of major radius (x) corresponding to the center of the resonant region. See Fig. 3. Symmetry for $\pm y$ is assumed. θ_1 and θ_2 are the angles between the minor radii, r_1 and r_2, and the x-axis. The heat which is first generated in the two resonant regions then is quickly distributed, by the flow of ions along the magnetic lines of force, to the volume between the torus-shaped magnetic surfaces with minor radii r_1 and r_2.

For r_2 and r_1 close together, the average power per unit volume to the resonant ions, of density $n(r)$, on a toroidal magnetic surface with minor radius r is simply

$$<P> = \frac{n(r)Zec}{B} \frac{R}{r|\sin\theta|} |E_+|^2 \ .$$ (10)

This same result, averaged over the tokamak cross-section, was already obtained by Adam and Samain [14].

A happy consequence of this rf heating is the appearance of a geometrical effect which favors the deposition of heat in the core (small r) of the tokamak plasma.

5. ELECTRON LANDAU AND TRANSIT-TIME DAMPING

Landau damping and transit-time damping both involve energy absorption by particles moving along $\vec{B}$ with the phase velocity of the wave, i.e., particles for which $\omega - k_{"}v_{"} = 0$. In Landau damping, the force on the particle due to the wave is $q\vec{E}$; for transit-time damping the acting force is $-\mu\nabla B$. Both processes are effective in fast-wave damping by the thermal electrons. The exact calculation is tedious in its algebra as the two effects are coherent and cross-terms need be retained. Symbolically, the power abosrbed per unit volume is given simply by

$$P = - \frac{i\omega}{16\pi} \vec{E}* \cdot \vec{K} \cdot \vec{E} + \text{complex conjugate} \ ,$$

in which $\vec{E}$ is the complex amplitude in the representation of the real wave field $\vec{E}_o$, $\vec{E}_o = \text{Re}\{\vec{E} \exp(-i\omega t+i\vec{k}\cdot\vec{r})\}$, and $\vec{K}$ is the

usual hot plasma dielectric tensor. The only terms of $\vec{K}$ that need be retained in the expression for P are the collisionless absorption terms from the $\omega - k_{\shortparallel} v_{\shortparallel} = 0$ electron resonance,

$$P = - \frac{i\omega}{8\pi} [|E_y|^2 \Delta K_{yy} - 2i|E_y E_z| \sin\alpha \Delta K_{yz} + |E_z|^2 \Delta K_{zz}], \quad (11)$$

where we have made use of the Onsager relation $K_{yz} = -K_{zy}$, and where

$$\Delta K_{yy} = \frac{i}{|\omega_{ce}|} \frac{k_x^2 s^2}{\omega} G \quad , \quad (12)$$

$$\Delta K_{yz} = \frac{k_x}{k_z} G \quad ,$$

$$\Delta K_{zz} = \frac{2i\omega|\omega_{ce}|}{k_z^2 s^2} G \quad ,$$

$$G \equiv \pi^{1/2} \frac{\omega_{pe}^2}{|\omega_{ce}|} \frac{1}{|k_z|s} \exp(-\frac{\omega^2}{k_z^2 s^2}) \quad ,$$

$$s^2 \equiv \frac{2kT_e}{m_e} \quad , \quad \frac{E_y}{E_z} = \left|\frac{E_y}{E_z}\right| e^{i\alpha} \quad .$$

The evaluation of the amplitude and phase relations between E_y and E_z is made in a straightforward fashion from the vector wave equation, Eq. (1), using the hot-electron forms for $\vec{K}$ including K_{yz} and K_{zy}. The calculation is simplified in the

weak-damping limit in that it suffices to retain only the reactive elements in $\vec{K}$. From the x and z components of the wave-equation one derives

$$\frac{E_y}{E_z} = \frac{(n_x n_z)^2 - (K_{xx} - n_z^2)(K_{zz} - n_x^2)}{-n_x n_z K_{xy} + (K_{xx} - n_z^2) K_{zy}} \quad . \tag{13}$$

K_{xx} and K_{xy} involve mainly ions and the cold-plasma forms may be used. $K_{zz} = -\omega_{pe}^2/\omega^2$ or $(k_z^2 \lambda_D^2)^{-1}$ when $(\omega/k_{\shortparallel}s)^2 \gg 1$ and $(\omega/k_{\shortparallel}s)^2 \ll 1$ respectively, and $K_{zy} = 0$ or $ik_x \omega_{pe}^2/(k_z \omega |\omega_{ce}|)$ in the same two limits respectively. If desired, one may use $B_z = (k_x c/\omega) E_y$ to express the transit-time damping in terms of the wave B_z-field.

Eq. (13) is of interest to us in this application only when Landau or transit-time damping are not negligible. In such regimes $(\omega/k_{\shortparallel}s) \lesssim 1$, and the K_{zy} term in the denominator will dominate. Then we may reasonably approximate

$$\frac{E_y}{E_z} \simeq -\frac{K_{zz}}{K_{zy}} = i \frac{\omega e B}{k_x k_z k T_e c} \quad . \tag{14}$$

For low frequencies, a simple argument gives the same result. Say ions move in and out with $\vec{B}$ — then by quasineutrality, $n_e \sim B_z$. Also, for hot electrons, $n_e = n_o \exp(e\phi/kT_e)$. Finally, using the induction equation, $\partial B_z/\partial t = -c\partial E_y/\partial x$, the above relation follows.

It is particularly interesting to observe that the substitution of this phase and amplitude relationship for E_y and E_z leads to exact cancellation between the transit-time term (ΔK_{yy}) and the cross-term (ΔK_{yz}), leaving only the Landau damping term (ΔK_{zz}) which is then equal in magnitude to one-half of the

transit-time term,

$$P_{total} \simeq - \frac{i\omega}{16\pi} \Delta K_{yy} |E_y|^2 \quad . \tag{15}$$

6. WAVE ENERGY DENSITY

A convenient way to compute the wave damping rate is to divide the power absorption by the wave energy density, W. From conventional wave theory,

$$W = \frac{1}{16\pi} [\vec{B}^* \cdot \vec{B} + E^* \cdot \frac{\partial}{\partial \omega} (\omega \vec{K}_h) \cdot \vec{E}] \quad , \tag{16}$$

where $\vec{K}_h$ is the Hermitian portion of the dielectric tensor. With the cold-plasma dielectric tensor elements, and making use of the phase relation between E_x and E_y derived from Eq. (1), we find

$$W = \frac{1}{16\pi} \cdot \frac{4\pi n_i m_i c^2}{B^2} \{N_{\parallel}^2 (H^2+1) + N_{\perp}^2 \tag{17}$$

$$+ \frac{A^2}{2} [(1+H)^2 (1-\frac{\omega}{\omega_{ci}})^2 + (1-H)^2 (1+\frac{\omega}{\omega_{ci}})^2]\} |E_y|^2 \quad ,$$

$$H \equiv \frac{iE_x}{E_y} = - \frac{\omega_{ci}}{\omega} \cdot \frac{N_{\perp}^2 + N_{\parallel}^2 - A}{A} \quad , \quad A \equiv \omega_{ci}^2 / (\omega_{ci}^2 - \omega^2) \quad .$$

$N_{\parallel}^2$ and $N_{\perp}^2$ are related, of course, by the dispersion relation in Eq. (3). The first two terms inside the brackets represent magnetic field energy, and the A^2 term is the kinetic energy of the coherent particle motion.

7. AN EXAMPLE

To illustrate the calculations presented here, we look at one representative case, a tokamak plasma with the following parameters:

Triton density $n_T = 5 \times 10^{13}$ cm^{-3}

Deuteron density $n_D = 2.5 \times 10^{12}$ cm^{-3}

Temperature $kT_i = kT_e = 4000$ eV

Magnetic field   40 kG

Major radius   274 cm

Minor radius   60 cm

Wave frequency $\omega = \omega_c$(deuterons)$= 2\pi(30.5)$ MHz

Parallel wavelength $\lambda_{\shortparallel} = 123$ cm

The first group of computations concerns the background plasma, and the deuteron contribution is neglected.

$$\frac{4\pi n_i m_i c^2}{B^2} = 1770 \ .$$

$$(2kT_e/m_e)^{1/2} = 3.75 \times 10^9 \text{ cm/sec}$$

$$(2kT_i/m_i)^{1/2} = 5.06 \times 10^7 \text{ cm/sec}$$

$$(\omega/k_{\shortparallel})(2kT_e/m_e)^{-1/2} = 1$$

$n_z = 7.99$

$N_{\shortparallel}^2 = 0.0362$

$n_x = 39.6$

$\lambda_x = 2\pi/k_x = 24.8$ cm

$N_{\perp}^2 = 0.886$

$\omega/\omega_c = 1.50$

$A = -0.8$

$K_{xx} \approx K_{yy} = -1410$

$K_{xy} = -K_{yx} = -i2120$

$R = 707$

$L = -3530$

$$K_{zy} = -K_{yz} = -3810 - i445$$

$$K_{zz} = -6.60 \times 10^5 + i5.65 \times 10^6$$

$$\Delta K_{yy} = i5.14$$

$$\Delta K_{yz} = 3810$$

$$\Delta K_{zz} = i5.65 \times 10^6$$

$$H = 1.435$$

$$W = 65.0 |E_y|^2 \quad (54\% \text{ magnetic, } 46\% \text{ kinetic})$$

$$|E_y/E_z| = 1.453 \times 10^3$$

$$\alpha = 83.4°$$

$$G = 3670$$

$$E_+/E_- = 0.179$$

$$E_+/iE_y = -0.218$$

$$\text{Volume} = 1.947 \times 10^7 \text{ cm}^3$$

The power computations show

$$P_{\text{transit-time}}(\Delta K_{yy}) = 3.92 \times 10^7 |E_y|^2 \text{sec}^{-1}$$

$$P_{\text{cross-terms}}(\Delta K_{yz}) = -3.97 \times 10^7 |E_y|^2 \text{sec}^{-1}$$

$$P_{\text{Landau}}(\Delta K_{zz}) = 2.04 \times 10^7 |E_y|^2 \text{sec}^{-1}$$

$$P_{\text{Total}}(\text{electrons}) = 1.99 \times 10^7 |E_y|^2 \text{sec}^{-1}$$

$$Q(\text{electrons}) \equiv \omega W/P_{\text{total}} = 628$$

With the addition of 5% deuterons and electrons, both at $kT = 4000$ eV, we compute

$$\Delta R(\text{deuterons plus electrons}) = 29.5$$

$$\Delta L(\text{electrons}) = -59.0$$

$$\Delta L(\text{deuterons}) = i6330.$$

$$E_+/E_- = 0.0920 \; \underline{/60.0°}$$

$$E_+/iE_y = 0.0961 \; \underline{/-115.3°}$$

We assume the central resonant surface passes through magnetic axis.

Then $\sin\theta = 1$ in Eq. (10), and the power absorbed per unit volume is

$$P = 8.32 \times 10^6 (R/r) |E_y|^2 \ \text{sec}^{-1}$$

$$<P> \equiv (2/a^2) \int_o^a P(r) r dr, \ \text{for} \ |E_y|^2 = \text{const},$$

$$= 7.60 \times 10^7 |E_y|^2$$

$$Q(\text{ions}) = \omega W/<P> = 164 \ .$$

The kinetic energy of the deuterons has not been included in W in the last expression; its inclusion will increase $Q(\text{ions})$. However, the small fraction of deuterons present and the unfavorable polarization of $\vec{E}$ will limit the size of this contribution.

8. QUASILINEAR DIFFUSION COEFFICIENTS

Generally in rf heating applications it is sufficient to know just the rate of power absorption from a wave of given amplitude. For creating a fusion-producing ion tail, however, we want to know precisely how the ion velocity distribution is affected. The means for this computation are readily available by including the quasi-linear diffusion coefficient among the Fokker-Planck terms in the Boltzmann equation. The quasilinear diffusion coefficient for cyclotron absorption was calculated by Kennel and Engelmann [15], and in the absence of other diffusive processes, the kinetic ion equation reads

$$\frac{\partial f(\vec{v})}{\partial t} = \lim_{V \to \infty} \sum_n \frac{\pi z^2 e^2}{m^2} \int \frac{d^3\vec{k}}{(2\pi)^3 V} \ L\dot{v}_\perp \delta(\omega - k_{\shortparallel} v_{\shortparallel} - n\omega_{ci}) \ |\Theta_{n,k}|^2 v_\perp L f$$

(18)

where

$$L \equiv (1 - \frac{k_{\shortparallel} v_{\shortparallel}}{\omega}) \frac{1}{v_\perp} \frac{\partial}{\partial v_\perp} + \frac{k_{\shortparallel}}{\omega} \frac{\partial}{\partial v_{\shortparallel}} \ ,$$

$$\theta_{n,k} = \frac{1}{2} e^{i\psi}(E_x - iE_y)_k J_{n+1}\left(\frac{k_\perp v_\perp}{\omega_{ci}}\right) + \frac{1}{2} e^{-i\psi}(E_x + iE_y)_k J_{n-1}\left(\frac{k_\perp v_\perp}{\omega_{ci}}\right)$$

$$+ \frac{v_{\shortparallel}}{v_\perp}(E_z)_k J_n\left(\frac{k_\perp v_\perp}{\omega_{ci}}\right) \qquad ,$$

$$\vec{k} = \hat{x}k_\perp\cos\psi + \hat{y}k_\perp\sin\psi + \hat{z}k_{\shortparallel} \qquad ,$$

V is the plasma volume, and $\vec{E}_k$ are the Fourier amplitudes in the usual complex analysis of the wave field. For present purposes we can drop the parallel velocity effects in the L operator, Eq. (18), but this point will be discussed at the end of this section. We may also neglect the E_z and $E_x - iE_y$ (right-handed) contributions to $\theta_{n,k}$, assume $\psi = 0$ and a monochromatic spectrum. Then, carrying out the integration in [18] over $\vec{k}$,

$$\frac{\partial f(\vec{v})}{\partial t} \simeq \frac{\pi Z^2 e^2}{8m^2|k_{\shortparallel}|} |E_x + iE_y|^2 \sum_n \frac{1}{v_\perp} \frac{\partial}{\partial v_\perp} v_\perp^2 \left|J_{n-1}\left(\frac{k_\perp v_\perp}{\omega_{ci}}\right)\right|^2 \delta\left[v_{\shortparallel} - \frac{(\omega - n\omega_{ci})}{k_{\shortparallel}}\right]\frac{1}{v_\perp}\frac{\partial f}{\partial v_\perp}$$

$$(19)$$

summed over the cyclotron harmonics. The electric field in (19) is $\vec{E} = \text{Re}(\hat{x}E_x + \hat{y}E_y)\exp(i\vec{k}\cdot\vec{r} - i\omega t)$. For acceleration at the cyclotron fundamental, the Bessel factor is $J_0(k_\perp v_\perp/\omega_{ci}) \to 1$ in the small Larmor-radius limit. To recover our previous result, Eq. (8), on ion heating, we simply integrate twice by parts,

$$2\pi \int v_\perp dv_\perp dv_{\shortparallel} \frac{mv^2}{2} \frac{\partial f}{\partial t} = 2\pi \int v_\perp dv_\perp \left[\frac{\pi Z^2 e^2}{4m|k_{\shortparallel}|} |E_x + iE_y|^2 f(v_{\shortparallel}^{(res)})\right] \quad . (20)$$

For comparison with (8) and (10), we observe that $|E_x + iE_y|^2 = 4|E_+|^2$.

Two points of general interest now come up which concern
the use of the quasilinear diffusion coefficients for the cyclo-
tron heating calculation. The first, already referred to in
Section 4, is that the direct calculation of resonant-ion heating
in the inhomogeneous magnetic field leads to the identical result,
Eq. (8), as the local use of the quasilinear diffusion coefficient,
Eq. (20), and that this identity of results therefore justifies
the use of this coefficient even though the electric field spectrum
is monochromatic. The critical consideration is that the usual
quasilinear calculation demands a spectrum of randomly phased
modes to justify the concept of true particle diffusion resulting
from a number of incoherent velocity displacements, whereas in
the present heating calculation we consider that the irradiation
is monochromatic in both frequency and wavenumber. The usual
problem for the monochromatic spectrum is that wave-particle phase
relations can be altered by the very coherence of the wave, as
when trapping occurs. However, this difficulty is easily avoided
in the tokamak heating provess under consideration. In each passage
through the resonant surface the particles here pick up small in-
crements to their perpendicular velocity and to justify the descrip-
tion of this process as velocity-space diffusion we require just
that successive velocity increments be randomly phased, i.e., that
$u(-\infty)$ in the Section 4 calculation be randomly phased with respect
to the oscillating electric field. The necessary randomness easily
appears from collisions — the collision rate need only be such that
particles "forget" the phase of the cyclotron heating field
between successive transits of the resonant surface. Typically
the time between successive transits will be the time for an ion to

execute half a poloidal rotation in a tokamak, $\tau_p \approx \pi R q / v_\shortparallel$. The
irreproducibility in τ_p will be $\Delta\tau_p \approx \pi R q (\Delta v_\shortparallel)/v_\shortparallel^2$, and
dispersion by Coulomb scattering will lead to rms $\Delta v_\shortparallel$ values of
order $(<(\Delta v_\shortparallel)^2> \tau_p)^{1/2}$ after half a poloidal rotation. Requiring
that ions "forget" the cyclotron phase between transits just says
that $\omega_{ci}\Delta\tau_p >> 1$, or that

$$\frac{<(\Delta v_\shortparallel)^2>}{v_\shortparallel^2} >> \frac{1}{(\omega_{ci}\tau_p)^2} \frac{1}{\tau_p}$$

The diffusion coefficient $<(\Delta v_\shortparallel)^2>$ is evaluated in
Eq. (28) in this paper, and the randomization criterion can be
seen to be very easily satisfied in actual tokamaks, even in the
ion banana regime.

The second point of general interest in this quasilinear
diffusion calculation is that cyclotron heating is generally
considered a process which causes dispersion only in $v_\perp$. However,
a look at the structure of the diffusion operator, L, shows that
dispersion in parallel velocities is also involved. In fact, the
L operator is a gradient operator in velocity space directed along
the circle

$$v_\perp^2 + (v_\shortparallel - \frac{\omega}{k_\shortparallel})^2 = \text{constant}$$

and quasilinear diffusion takes place only along these circles,
Fig. 4. The sketch illustrates that the amount of parallel diffusion
occurring under cyclotron resonance can be appreciable. It must be
remembered, however, that resonant particles are involved, so the
diffusion occurs on the circles only where they intersect the line

$v_\parallel = (\omega - n\omega_{ci})/k_\parallel$, and the slope of the curves away from this intersection does not have physical meaning.

9. FOKKER-PLANCK EQUATION

We now want to write down a kinetic equation for the ion velocity distribution incorporating the combined effects of quasilinear heating and Coulomb thermalization. A convenient form for the Fokker-Planck equation is

$$\frac{\partial f}{\partial t} = -\nabla_v \cdot (<\Delta\vec{v}>f) + \frac{1}{2} \nabla_v \cdot [\nabla_v \cdot (<\Delta\vec{v}\Delta\vec{v}>f)] \ , \tag{21}$$

the first term representing drag, the second term dispersion. We will be satisfied to examine the evolution of the distribution function for a small number of ions (e.g., a small minority component of deuterons in a thermal triton plasma, or the high-energy non-Maxwellian ion tail thermalizing against an approximately Maxwellian ion body distribution) and ask only for the Fokker-Planck coefficients for test particles diffusing in an isotropic Maxwellian plasma of ions and electrons. The needed Coulomb coefficients are those of Chandrasekhar and Spitzer [16], given for Cartesian coordinates in velocity space as $<\Delta v_\parallel>$, $<(\Delta v_\parallel)^2>$ and $<(\Delta v_\perp)^2>$. (For these Coulomb coefficients, $\perp$ and $\parallel$ denote directions with respect to the test-particle $\vec{v}$, and do not pertain to $\vec{B}$.) Going to spherical coordinates in velocity space and adding the quasilinear diffusion to the Coulomb terms [17], the total kinetic equation is

$$\frac{\partial f}{\partial t} = C(f) + Q(f) \qquad , \qquad (22)$$

$$C(f) \equiv -\frac{1}{v^2}\frac{\partial}{\partial v}[v^2(<\Delta v_{\shortparallel}> + \frac{1}{2v}<(\Delta v_{\perp})^2>)f]$$

$$+ \frac{1}{2v^2}\frac{\partial^2}{\partial v^2}(v^2<(\Delta v_{\shortparallel})^2>f)$$

$$+ \frac{1}{4v^2}\frac{\partial}{\partial \mu}(1-\mu^2)\frac{\partial}{\partial \mu}(<(\Delta v_{\perp})^2>f) \quad ,$$

$$Q(f) \equiv \sum_{mn} Q_{mn}\delta(\omega_{ci} - \frac{(\omega-k_{\shortparallel}v_{\shortparallel})}{n})R_m(f) \quad ,$$

$$R_m(f) \equiv (1-\mu^2)^{m+1}\frac{1}{v^2}\frac{\partial}{\partial v}v^{2m+1}\frac{\partial}{\partial v}vf + v^{2m-2}\frac{\partial}{\partial \mu}\mu(1-\mu^2)^{m+1}\frac{\partial}{\partial \mu}\mu f$$

$$- v^{2m-2}\frac{\partial}{\partial \mu}\mu(1-\mu^2)^{m+1}\frac{\partial}{\partial v}vf$$

$$- (1-\mu^2)^{m+1}v^{2m-2}\frac{\partial}{\partial \mu}\mu\frac{\partial}{\partial v}vf - 2m(1-\mu^2)^{m+1}v^{2m-2}\frac{\partial}{\partial \mu}\mu f \quad ,$$

where $Q_{mn}(\vec{r})$ is the coefficient of $v_{\perp}^{2m}$ in the power series

$$\sum Q_{mn} v_{\perp}^{2m} = \frac{\pi Z^2 e^2}{8m_i^2|n|}|E_x+iE_y|^2|J_{n-1}(\frac{k_{\perp}v_{\perp}}{\omega_{ci}})|^2 \quad , \qquad (23)$$

where μ is the cosine of the angle in velocity space between $\vec{v}$ and $\vec{B}$, and where we have used the relation for differentiation with respect to $v_{\perp}^2 = v^2(1-\mu^2)$,

$$\frac{\partial}{v_{\perp}\partial v_{\perp}} = \frac{1}{v^2}(\frac{\partial}{\partial v}v - \frac{\partial}{\partial \mu}\mu) \quad .$$

Since ω_{ci} is a function of the major radius in a tokamak, we can eliminate the delta function in Eq. (22) by averaging over a toroidal magnetic surface of minor radius r, major radius R, as in the derivation of Eq. (10),

$$\frac{1}{2\pi} \int d\theta \, Q_{mn}(x,y) \delta [\omega_{ci} - \frac{(\omega - k_{\shortparallel} v_{\shortparallel})}{n}] \tag{24}$$

$$\approx \frac{R}{\pi \omega_{ci} r |\sin\theta_0|} Q_{mn}(x_0, |y_0|) \quad ,$$

where $\theta_0 = \tan^{-1}(|y_0|/x_0)$, and x_0, y_0 are the coordinates in the plasma cross-section where the selected magnetic surface intersects the central $(v_{\shortparallel} = 0)$ resonant surface. Compare Fig. 3. We have assumed that the cross-section of the magnetic surface is a circle centered around $(x,y) = (0,0)$, that $f = f(r,\vec{v})$, independent of the spatial angle θ, and that $Q_{mn}(x,y)$ is symmetric for $y = \pm|y_0|$ and is well approximated over the resonant interaction region by its central value at $x = x_0$.

10. EXPANSION OF $f(\vec{v})$ IN LEGENDRE POLYNOMIALS

The conventional way to obtain an analytic solution to a partial differential equation such as Eq. (22) is by the expansion of f in a series of Legendre polynomials in μ,

$$f(r,\vec{v},t) = \sum_{\ell=0}^{\infty} g_{2\ell}(r,v,t) P_{2\ell}(\mu) \quad .$$

For $Q(f) = 0$, the expansion is particularly appropriate since the $P_k(\mu)$ are eigenfunctions of the $C(f)$ operator. $Q(f) \neq 0$

unfortunately mixes the various $P_k(\mu)$ functions, but the expansion is still useful because the μ integrations are easy, and the problem is quickly reduced to a set of coupled linear differential equations in v and t. Restricting our attention to the case for heating at the fundamental cyclotron frequency ($n = 1$), and keeping only the first two terms in the μ-expansion,

$$f(v,t) = A(v,t) + \frac{1}{2}B(v,t)(3\mu^2-1) ,$$

we obtain from the $P_o(\mu)$ and $P_2(\mu)$ moments of Eq. (22)

$$\frac{\partial A}{\partial t} = \frac{1}{v^2} \frac{\partial}{\partial v}[-\alpha v^2 A + \frac{1}{2} \frac{\partial}{\partial v}(\beta v^2 A) \qquad (25)$$

$$+ Kv \frac{\partial}{\partial v} v(A - \frac{B}{5}) - K(A + \frac{2}{5}B)v]\qquad ,$$

$$\frac{\partial B}{\partial t} = - \frac{1}{v^2} \frac{\partial}{\partial v}(\alpha v^2 B) + \frac{1}{2v^2} \frac{\partial^2}{\partial v^2} (\beta v^2 B) - \frac{3}{2} \frac{\gamma}{v^2} B$$

$$+ \frac{K}{v^2} \frac{\partial}{\partial v} v \frac{\partial}{\partial v} v[-A + \frac{5}{7} B] - \frac{K}{v^2}[3A + \frac{30}{7} B]$$

$$+ \frac{K}{v^2} \frac{\partial}{\partial v} v[4A - \frac{5}{7} B] \qquad , \qquad (26)$$

in which, using Eqs. (10), (23), and (24),

$$K \equiv \frac{2R}{3\pi\omega_{ci}r|\sin\theta_o|} \, Q_{01}(x_o,|y_o|) = \frac{<P>}{3n_im_i} \quad , \qquad (27)$$

$$\alpha \equiv <\Delta v_{\shortparallel}> + \frac{1}{2v} <(\Delta v_{\perp})^2> \quad ,$$

$$\beta \equiv <(\Delta v_{\shortparallel})^2> \quad ,$$

$$\gamma \equiv <(\Delta v_{\perp})^2> \quad .$$

11. THE COULOMB DIFFUSION COEFFICIENTS

The Coulomb diffusion coefficients are given in Spitzer [16]. We use subscript f to designate the background-plasma field particles, ions and electrons,

$$<\Delta v_{\shortparallel}> = - \sum_f C_f \, \ell_f^2 (1 + \frac{m}{m_f}) G(\ell_f v) \quad ,$$

$$<(\Delta v_{\shortparallel})^2> = \sum \frac{C_f}{v} G(\ell_f v) \quad ,$$

$$<(\Delta v_{\perp})^2> = \sum_f \frac{C_f}{v} [\Phi(\ell_f v) - G(\ell_f v)] \quad , \qquad (28)$$

$$C_f \equiv \frac{8\pi n_f Z_f^2 Z^2 e^4 \, \ell n \, \Lambda}{m^2} \quad ,$$

$$\ell_f^2 \equiv m_f/2kT_f \qquad ,$$

$$\Phi(x) \equiv \frac{2}{\pi^{1/2}} \int_0^x \exp(-y^2 \, dy) \quad ,$$

$$G(x) \equiv \frac{\Phi(x) - x\Phi'(x)}{2x^3} \quad .$$

In working with these diffusion coefficients, we will find the following identity useful,

$$-\alpha v^2 + \frac{1}{2} \frac{d}{dv}(\beta v^2) = \sum_f C_f \frac{mv^2}{2kT_f} G(\ell_f v) \qquad (29)$$

In addition, we introduce simple approximations to the somewhat cumbersome G and Φ functions. Both approximations produce the correct leading terms in the two limits of small and large x; in midrange, at the points of maximum fractional error, $G(1.819)$ is about 10.5% too low, while $\Phi(1.040)$ is about 27.4% too high. The two approximating forms are

$$G(x) \approx \varepsilon x/(1 + 2\varepsilon x^3) \quad , \qquad (30)$$

$$\Phi(x) \approx \varepsilon(3x + 2x^3)/(1 + 2\varepsilon x^3) \quad ,$$

$$\varepsilon \equiv 2/3\pi^{1/2} \quad .$$

It will be seen shortly that the use of these special forms permits the complete solution of the one-dimensional Fokker-Planck equation by elementary integrals. Meanwhile, the following more easily interpreted forms for the Coulomb diffusion coefficients may be derived from the preceding equations using just the leading terms for $G(x)$ and $\Phi(x)$,

	$\underline{\alpha}$	$\underline{\beta}$	$\underline{\gamma}$
Range I	D/v	D	$2D$
Range II	$-\frac{v}{t_s}(1 + \frac{v_\alpha^3}{v^3})$	$\frac{2kT_e}{mt_s}(1 + \frac{v_\beta^3}{v^3})$	$\frac{1}{t_s}\frac{v_\gamma^3}{v}$

where Range I is for $v \ll (2kT_i/m_i)^{1/2}$ and Range II for $(2kT_i/m_i)^{1/2} \ll v \ll (2kT_e/m_e)^{1/2}$, and where, summing over the f species of field ions and electrons,

$$D \equiv \varepsilon \sum_f C_f \ell_f$$

$$= 2 \sum_f \frac{n_f z_f^2}{n_e} \left(\frac{m_f T_e}{m_e T_f}\right)^{1/2} \frac{kT_e}{mt_s} \quad ,$$

$$t_s \equiv \frac{m_e}{\varepsilon m C_e} \left(\frac{2kT_e}{m_e}\right)^{3/2}$$

$$= 6.27 \times 10^8 \frac{A(kT_e)^{3/2}}{z^2 n_e \ \ell n \ \Lambda} \quad \text{seconds} \quad .$$

Summing over the j species of field ions,

$$\frac{1}{2} m v_\alpha^2 = 14.8 \ kT_e \left[\frac{A^{3/2}}{n_e} \sum_j \frac{n_j z_j^2}{A_j}\right]^{2/3} \quad , \tag{31}$$

$$\frac{1}{2} m v_\beta^2 = 14.8 (kT_e)^{1/3} \left[\frac{A^{3/2}}{n_e} \sum_j \frac{n_j z_j^2 kT_j}{A_j}\right]^{2/3} \quad ,$$

$$\frac{1}{2} m v_\gamma^2 = 14.8 \ kT_e \left[\frac{2A^{1/2}}{n_e} \sum_j n_j z_j^2\right]^{2/3} \quad .$$

A and A_j are the atomic masses of the test and field ions, n_e is in cm^{-3}, and kT_e in eV.

12. STEADY-STATE $f(v,\mu)$, LOWEST ENERGY RANGE

Now armed with explicit forms for the diffusion coefficients, we can look for solutions to the Fokker-Planck equation for the

rf-heated resonant ions. In most rf-heating experiments, the experimentalist is able to irradiate the plasma with an rf pulse of sufficient duration that the temperatures reach a steady-state value or, due to impurity influx, may even start to droop. It is meaningful then to look for steady-state solutions to Eq. (22) or Eqs. (25) and (26). It should be noted, however, that the occurrence of a steady-state solution is peculiar to heating at the fundamental cyclotron frequency. $n\underline{\underline{th}}$ -harmonic cyclotron heating would replace K in the integral of Eq. (31) by a quantity proportional to $Kv^{2n}+...,$ as required by Eqs. (22) and (23), and the calculated distribution function will no longer give convergent number and energy densities. Physically, harmonic heating acts preferentially on the higher-energy, larger-Larmor-radius particles, and if unchecked, leads to time-dependent runaway of their energy.

For thermal energies and above, the full determination of $f(v,\mu)$ probably requires computer analysis, but in the lowest energy range, i.e., for $v << (2kT_i/m_i)^{1/2}$, the diffusion coefficients are sufficiently simple that an explicit solution to Eqs. (25) and (26) is easily obtained. In steady-state, $\partial A/\partial t = 0$ and Eq. (25) can be integrated one time immediately. Furthermore, the condition that A and its derivatives vanish as $v \to \infty$ requires that the constant of integration be zero. Then using identity (29) and the Range I approximations for $\alpha,$ β and $\gamma,$ we find

$$A = \text{constant}\cdot\exp-(mv^2/2kT_{eff}) \quad,$$

$$kT_{eff} = (D + 2K)/[\epsilon \sum_f (C_f \ell_f/kT_f)]$$

$$B = \frac{4K}{7D + 10K} \left(\frac{mv^2}{2kT_{eff}}\right)^2 A$$

The f-sum, again, is over background ions and electrons. When all T_f are equal, $T_f = T_o$, then $kT_{eff} = (D + 2K)kT_o/D$. And further, when $K \to 0$, then $T_{eff} \to T_o$ and $B \to 0$. When $K \neq 0$, the resonant-ion velocity distribution is still approximately Maxwellian for the lowest range of velocities, but with an effective temperature above that of the background ions and electrons. A curious artifact of this $K \neq 0$ solution is that the constant-$f(\vec{v})$ surfaces near the origin of velocity space are <u>prolate</u> spheroids around the $\vec{B}$ direction even though the applied wave-diffusion introduces dispersion in $v_\perp$. Were it not for a certain cancellation of terms in Eq. (26) when A is of the Maxwellian form, the lowest term for B would be $B \sim -v^2 A$ and the corresponding constant-$f(\vec{v})$ surfaces would be the expected oblate spheroids.

As indicated earlier, the complexity of the diffusion coefficients makes the full determination of $f(v,\mu)$ much more difficult at thermal energies and above. Nevertheless, a very useful estimate of the magnitude of the angular dependence may be obtained by integration of Eq. (26) over $v^2 dv$ from 0 to ∞. The only surviving terms are

$$\int_0^\infty \left(\frac{\gamma(v)}{2} + \frac{10}{7} K\right) B(v)\, dv = - K \int_0^\infty A(v)\, dv \qquad (32)$$

which suggests that

$$B(v) \sim - KA(v) / [\frac{\gamma(v)}{2} + \frac{10}{7}K] \quad ,$$

as a very rough estimation. We note that the indicated ellipticity is, happily in this case, oblate, proportional to K for small K, and that B/A approaches a constant negative value for large K. (The expansion in Legendre poloynomials for the extreme case of a thin-disc distribution function, $f(\vec{v}) \sim \delta(\mu)$, would lead to the value -5/4 for the ratio of the coefficient of $P_2(\mu)$ to that of $P_0(\mu)$.)

The use of just two terms in the $P(\mu)$ expansion is a rather unsatisfactory way to represent the angular dependence of $f(\vec{v})$ when K is large. Additional terms could be included, at the obvious cost of increasing analytic complexity, but for the large-K case it is worthwhile to explore the alternative representation of the Fokker-Planck equation using $v_\perp, v_\parallel$ as variables rather than v, μ. We will discuss the $v_\perp, v_\parallel$ representation in some detail in Section 14.

13. STEADY-STATE f(v) SOLUTION

The determination of the resonant-ion velocity distribution function is impressively simplified if we drop angular dependence from the model. The expansion of the Fokker-Planck equation, truncated at $f(\vec{v}) = A(v) = (1/2) \int f(v,\mu) d\mu$, is then just Eq. (25) with $B = 0$ and it is immediately integrable,

$$f(v) = f(0) \exp - \int_0^v dv \; \frac{-2\alpha v^2 + (\beta v^2)'}{\beta v^2 + 2Kv^2} \quad . \tag{33}$$

The Coulomb diffusion coefficients α and β are given in (27) and (28), and identity (29) provides a convenient form for the numerator of the integrand. For the background electron contributions to $G(x)$ it suffices to use $G(x_e) \approx \varepsilon x_e$ since in the velocity range of interest $v \ll (2kT_e/m_e)^{1/2}$. We assume a single species of background ions with density, temperature and charge n_j, T_j, and $Z_j e$, and use the approximating form for $G(x_j)$ offered in (30). Algebraic manipulation of the integrand then leads to the explicit solution for $f(v)$,

$$\ln f(v) = -\frac{E}{kT_e(1+\xi)}\left[1 + \frac{R_j(T_e-T_j+\xi T_e)}{T_j(1+R_j+\xi)} H(E/E_j)\right] \tag{34}$$

$$E \equiv mv^2/2, \qquad \ell_j \equiv (m_j/2kT_j)^{1/2},$$

$$R_j \equiv n_j Z_j^2 \ell_j/n_e \ell_e, \qquad \varepsilon \equiv 2/3\pi^{1/2},$$

$$\xi \equiv 2K/\varepsilon C_e \ell_e = \frac{\dot{m}\langle P\rangle}{8\pi^{1/2}n_e n Z^2 e^4 \ln \Lambda}\left(\frac{2kT_e}{m_e}\right)^{1/2},$$

$$E_j(\zeta) \equiv \frac{mkT_j}{m_j}\left[\frac{1+R_j+\xi}{2\varepsilon(1+\xi)}\right]^{2/3} \leqslant E_j(0),$$

$$E_j(0) = \frac{1}{2}mV_\beta^2, \quad \text{cf. Eq. (31)},$$

$$H(x) \equiv \frac{1}{x}\int_0^x \frac{du}{1+u^{3/2}}$$

$$= \frac{2}{x}\left[\frac{1}{6}\ln\frac{1-x^{1/2}+x}{1+2x^{1/2}+x} + \frac{1}{3^{1/2}}\left(\frac{\pi}{6} + \tan^{-1}\frac{2x^{1/2}-1}{3^{1/2}}\right)\right]$$

$$\approx 1 - \frac{2}{5}x^{3/2} + \frac{1}{4}x^3 - \frac{2}{11}x^{9/2} + \ldots$$

$$\approx 2.4184x^{-1} - 2x^{-3/2} + \frac{1}{2}x^{-3} - \frac{2}{7}x^{-9/2} + \ldots$$

Intermediate pairs of values for x,H(x) are 0.1, 0.9876; 0.2, 0.9661; 0.4, 0.9124; 0.7, 0.8263; 1, 0.7471; 2, 0.5544; 4, 0.3619; 7, 0.2389, and 10, 0.1791.

Z, m, n and v designate the charge number, mass, density and velocity of the resonant (test) ions. The effect of wave heating appears through the single dimensionless parameter ξ which is directly proportional to $<P>$, the wave-heating power per unit volume delivered to the test ions, averaged over a magnetic surface.

To discuss the behavior of f(v) in Eq. (34), it is useful to define an effective temperature at each value of $E = mv^2/2$, $kT_{eff} \equiv -[d(\ell n \, f)/dE]^{-1}$,

$$\frac{1}{kT_{eff}} = \frac{1}{kT_e(1+\xi)} \left[1 + \frac{R_j(T_e - T_j + \xi T_e)}{T_j(1+R_j+\xi)} \cdot \frac{1}{1+(E/E_j)^{3/2}}\right] \, .$$

For $\xi = 0$ the body of the test-ion distribution is Maxwellian with temperature very close to that of the background ions $(kT_{eff} \approx kT_j)$, while the tail of the test-ion distribution $(E \geqslant E_j)$ is influenced by the background electrons. For $\xi > 0$, kT_{eff} for $E << E_j(\xi)$, identical to kT_{eff} derived earlier in Section 12, is somewhat above the background ion temperature. As E increases, the effective temperature increases and, for $E >> E_j(\xi)$, kT_{eff} approaches the asymptotic value $kT_e(1+\xi)$ at which the wave-induced test-ion dispersion is entirely balanced by electron drag.

Plots of $\ell n \, f(v)$ versus E are shown in Fig. 5 for the parameters of the example introduced earlier, using $n_j z_j^2/n_e = 3$

for a $Z_{eff} = 3$ in computing R_j. For these same parameters,
the wave-induced dispersion level $\xi = 100$ corresponds to

1.3 watts per cm^3 rf power input to the plasma, averaged

over a magnetic surface. Maintaining this average power level

over the full volume of the model plasma in Section 7 would

require a total rf power input of 24 megawatts.

14. STEADY-STATE $f(v_\perp)$ SOLUTION

Our efforts to determine the angular dependence of $f(\vec{v})$
were fully successful only in the sub-thermal range of ion velocities,
although the integral relation (32) provides a useful estimate
of the anisotropy at thermal energies and above. However, at
the very high energies in the tail of the two-component plasma,
specifically, at test-ion energies above $\sim mv_\alpha^2/2$, the dominant
Coulomb process is electron drag which does not introduce apprecia-
ble pitch-angle scattering. Of especial interest is that the
perpendicular energy acquired from cyclotron heating is not shared
with the parallel degree of freedom, so that the coefficient of
wave-induced dispersion is increased by 50% throughout this energy
range.

To describe the strongly anisotropic velocity distribution
expected at high energies, it is fitting to change from v, μ
coordinates in velocity space to $v_\perp$, $v_{\shortparallel}$ coordinates. In the
new variables, the Coulomb terms in Eq. (22) are more intricate
but the quasilinear term reverts to the simpler form seen in Eq. (19).
The test-ion Fokker-Planck equation becomes

$$\frac{\partial f(v_\perp, v_\shortparallel, t)}{\partial t} = - \frac{1}{v}(v_\perp \frac{\partial}{\partial v_\perp} + v_\shortparallel \frac{\partial}{\partial v_\shortparallel} + 2)(\alpha f) \tag{35}$$

$$+ \frac{1}{2v^2}(v_\perp^2 \frac{\partial^2}{\partial v_\perp^2} + 2v_\perp v_\shortparallel \frac{\partial^2}{\partial v_\perp \partial v_\shortparallel} + v_\shortparallel^2 \frac{\partial^2}{\partial v_\shortparallel^2} + 4v_\perp \frac{\partial}{\partial v_\perp} + 4v_\shortparallel \frac{\partial}{\partial v_\shortparallel} + 2)(\beta f)$$

$$+ \frac{1}{4v^2}(v_\shortparallel^2 \frac{\partial^2}{\partial v_\perp^2} - 2v_\perp v_\shortparallel \frac{\partial^2}{\partial v_\perp \partial v_\shortparallel} + v_\perp^2 \frac{\partial^2}{\partial v_\shortparallel^2} + \frac{v_\shortparallel^2 - v_\perp^2}{v_\perp} - 2v_\shortparallel \frac{\partial}{\partial v_\shortparallel})(\gamma f)$$

$$+ \sum_{m,n} Q_{mn} \delta(\omega_{ci} - \frac{(\omega - k_\shortparallel v_\shortparallel)}{n})\frac{1}{v_\perp} \frac{\partial}{\partial v_\perp} v_\perp^{2m+1} \frac{\partial f}{\partial v_\perp} \quad .$$

$v \equiv (v_\perp^2 + v_\shortparallel^2)^{1/2}$, Q_{mn} is defined in (23), and α, β, and γ are defined in (27). Equation (35) is equivalent to Eq. (22), but we now direct our attention to regions where the distortion is strong enough that $\langle v_\perp^2 \rangle \gg \langle v_\shortparallel^2 \rangle$ and order terms according to $v_\perp \gg |v_\shortparallel|$, $v_\perp \sim v$, $v_\shortparallel (\partial/\partial v_\shortparallel) \sim v_\perp(\partial/\partial v_\perp)$. We average Eq. (35) over a magnetic surface, using (24), then define

$$f(v_\perp) \equiv \int_{-\infty}^{\infty} f(\vec{v}) dv_\shortparallel$$

and integrate (35) over $v_\shortparallel$. After some further straightforward integrations by parts (some small care must be taken with the $v_\perp^2 \partial^2 (\gamma f)/4v^2 \partial^2 v_\shortparallel^2$ term), the dominant terms are found for a one-dimensional Fokker-Planck equation describing heating at the cyclotron fundamental frequency,

$$\frac{\partial f(v_\perp, t)}{\partial t} \approx - \frac{1}{v_\perp} \frac{\partial}{\partial v_\perp}(\alpha v_\perp f) + \frac{1}{2v_\perp} \frac{\partial^2}{\partial v_\perp^2}(\beta v_\perp f) + \frac{1}{4v_\perp} \frac{\partial}{\partial v_\perp}(\gamma f)$$

$$+ \frac{3}{2} \frac{K}{v_\perp} \frac{\partial}{\partial v_\perp} v_\perp \frac{\partial f}{\partial v_\perp} \quad . \tag{36}$$

Like Eq. (25), Eq. (36), with $\partial f(v_\perp, t)/\partial t = 0$, can be quickly integrated twice to yield a steady-state solution,

$$f(v_\perp) = f(0) \ \exp - \int_0^{v_\perp} dv_\perp \ \frac{-4\alpha v_\perp + 2(\beta v_\perp)' + \gamma}{2\beta v_\perp + 6Kv_\perp} \ . \qquad (37)$$

Apart from the 50% increase in K, already discussed, Eq. (37) differs from its counterpart, Eq. (33), by the presence of the pitch-angle scattering coefficient in the numerator of the integrand. Pitch-angle scattering, like dispersion and drag, reduces $v_\perp$ when $v_\perp^2 \gg \langle v_{\shortparallel}^2 \rangle$.

Following the same steps which led from (33) to (34), making use in this instance as well of the approximating form for $\Phi(x)$ in (30), we find

$$\ell n \ f(v_\perp) = \frac{-2E}{kT_e(2+3\xi)} \Big\{ 1 + \frac{R_j[(2A+A_j)(2+3\xi)T_e - 4AT_j]}{2AT_j(2+2R_j+3\xi)} \ H(E/E_j) \Big\} \ ,$$

$$\qquad (38)$$

$$E_j \equiv \frac{AkT_j}{A_j} \left[\frac{2+2R_j+3\xi}{2\varepsilon(2+3\xi)} \right]^{2/3} \ .$$

Apart from E_j, the quantities in (38) are defined as in (34). A and A_j are the atomic masses of the test and field ions, respectively.

It should be remembered that Eq. (38) only applies to the velocity range where $f(\vec{v})$ is strongly anisotropic. An estimate of the lower boundary for this range of $v_\perp$ can come from examining the numerator of the integrand in (37): the pitch-angle

scattering term is smaller in magnitude than the electron drag term when $v_\perp^3 > V_\gamma^3/4$, defined in Eq. (31). Above this value of test-ion velocity, where pitch-angle scattering becomes relatively weak, the main source of parallel energy to the distribution will be by its incidental transport as particles wave-diffuse upward in $v_\perp$ carrying their $v_{\shortparallel}$ with them. The argument suggests that while the perpendicular distribution in the tail is described by (38), the parallel distribution for these same particles might be characterized by $kT_{\shortparallel} \sim mV_\gamma^3/8$.

15. f(v) FOR STEADY-STATE ISOTROPIC ION INJECTION

It is interesting, for the purpose of comparison, to examine the velocity distribution which results from the Coulomb slowing-down and diffusion of a group of test ions injected at high energy (as energetic neutral atoms) into a tokamak plasma. We assume the injected beam is originally monoenergetic at $mv^2/2 = W$ and isotropic in its velocity distribution. To formulate a steady-state model, we also assume an ion sink at some much lower energy, W_s, which absorbs test ions at the same rate that the source emits them. The Fokker-Planck equation is again Eq. (25) with $\partial A/\partial t = 0$, $B = 0$, $K = 0$, and with a source term, $\sim v^{-2} \cdot \delta [v-(2W/m)^{1/2}]$, and a sink term, $\sim -v^{-2} \cdot \delta [v-(2W_s/m)^{1/2}]$, added to the right-hand side. The first integration is immediate, the delta functions integrating into step functions; introduction of an integrating factor facilitates the second integration. Enormous simplification of the result occurs when the background

ions and electrons have the same temperature, kT. Then $A_o = \text{constant} \cdot \exp{-mv^2/2kT}$ must satisfy the steady-state equation without sources or sinks, and this very solution in fact follows directly from $A_o = \text{constant} \exp - \int dv [2\alpha v^2 - (\beta v^2)'] / (\beta v^2)$ and Eqs. (27), (28) and (29). With source and sink as just described, the full solution in the range $W_s < mv^2/2 < W$ is

$$f(v) = \text{constant} \cdot \exp - \frac{mv^2}{2kT} \int dv \, (\exp \frac{mv^2}{2kT}) / \beta v^2$$

and use of the Range II approximation for β then leads to

$$f(v) \approx \text{constant} \cdot \exp - \frac{E}{kT} \int_0^E dU \, \frac{\exp(U/kT)}{1 + [U/E_j(0)]^{3/2}} \qquad (39)$$

provided both $E \equiv mv^2/2 \gg kT$ and $W_s < E < W$. For $E > W$, the upper limit in the integral is W. $E_j(0) = mV_\beta^2/2$ is defined in Eqs. (31) and (34). Moreover, for $kT_e = kT_j = kT$, Eq. (31) shows $V_\beta^2 = V_\alpha^2$, and provided the denominator in the integrand of (39) does not change significantly over a range of U, $\Delta U \sim kT$, the integral may be approximated

$$f(v) \approx \frac{\text{constant}}{v^3 + V_\alpha^3} \qquad (40)$$

which is the customary solution for the distribution of originally-monoenergetic test ions, from a calculation based on drag alone and neglecting dispersion.

A plot of Eq. (39) for 200 keV deuteron injection into a 4 keV temperature tritium plasma is shown for comparison in Fig. 5.

16. EFFICIENCY FOR PRODUCTION OF FUSION REACTIONS

A primary objective in two-component plasma research will be the production of abundant D-T nuclear reactions, hopefully matching or exceeding the rate per unit plasma volume required for an economic fusion reactor. Toward achieving this goal, rf heating can be helpful in heating the background plasma, in enhancing the fusion output in a primarily beam-injected two-component plasma, or in the production by rf alone of an energetic-tail two-component plasma. Having determined the expected resonant-ion velocity distribution for different levels of rf heating, we are in a position to calculate the rf power cost for a certain rate of fusion reactions.

The D-T nuclear power produced per unit volume is

$$P_n = 4\pi n_T W_n \int_0^\infty v^2 dv\ f(v)\ \sigma(v)\ v \tag{41}$$

where n_T is the tritium density, W_n the nuclear energy released per D-T fusion reaction, and $\sigma(v)$ the D-T cross-section as a function of the deuteron velocity. The rf power per unit volume is proportional to wave-induced dispersion, ξ. Taking this factor of proportionality from (34), we find the ratio, Q_{RF}, of nuclear power produced to rf power input

$$Q_{RF} = \frac{W_n \langle \sigma v \rangle n_T m_D (2kT_e)^{1/2}}{8\pi^{1/2} \xi\, m_e^{1/2} n_e e^4 \ln \Lambda} \quad . \tag{42}$$

The σv average is to be taken over the distribution of resonant ions (deuterons). Especially convenient in computer calculation here is Duane's fit [18] to the D-T fusion cross-section. For the conditions pertaining to the example of Section 7, that is, $kT = 4$ keV, using $Z_{eff} = 3$ in computing R_j, Eq. (34), and using $W_n = 22.4$ MeV, the computed Q_{RF} values are 0.20 for $\xi = 100$, 0.38 for $\xi = 30$, and 0.045 for $\xi = 10$. The maximum value for $\langle \sigma v \rangle / \xi$, for the same conditions, occurs for $\xi = 42$, at which value $Q_{RF} = 0.45$.

For comparison, we consider the injection into the same tritium plasma of I deuterons per cm^3 per second with energy E_o. The deuteron velocity distribution, in accordance with Eq. (40), is $f(v) = I/4\pi\alpha v^2$ for $mv^2/2 < E_o$, $f(v) = 0$ for $mv^2/2 > E_o$. Putting this distribution into (41) determines the nuclear power, while the injected power is simply IE_o. The ratio, Q_I, for nuclear power to injected power is then

$$Q_I = \frac{n_T W_n}{E_o} \int_{V_o}^{0} \frac{\sigma v}{\alpha} \, dv, \quad \frac{mV_o^2}{2} \equiv E_o \ .$$

With $Z_{eff} = 3$ in computing V_α^2, Eq. (31), and with $kT = 4$ keV, $Q_I = 0.42$ for $E_o = 100$ keV, 0.74 for $E_o = 150$ keV, and 0.81 for $E_o = 200$ keV. Comparing these two sets of Q values we see that the efficiency for fusion power production from a $Z_{eff} = 3$ two-component plasma produced by selective rf absorption comes within a factor of two with the corresponding efficiency for a neutral-injection system.

For $Z_{eff} = 1$, computation shows Q_{RF} values significantly greater than unity. Figure 6 is a plot of Q_{RF} versus rf power,

parameterized by ξ, for various electron temperatures, with $Z_{eff} = 1$ and temperature $T_j = 4$ keV for the background triton ions. The Q_{RF} values decrease for very high rf powers and for very large electron temperatures because too large a fraction of the deuteron distribution then appears in the far tail (E > 200 keV) past the maximum of the fusion cross-section.

Figure 7 illustrates the effect of changing Z_{eff} and also the effect of lowering the background ion temperature.

17. SUMMARY

We have examined in considerable detail the use of the fast hydromagnetic wave for heating large magnetically-confined toroidal plasmas. Landau and transit-time damping, which are coherent processes, can couple power effectively into the electrons while the ions can be rf-heated with high efficiency at the second harmonic of their cyclotron frequency or at the fundamental cyclotron frequency of a minority ion species. In a particular application of the latter principle, selective rf absorption by deuterons in a predominantly triton plasma can lead to a two-component velocity distribution suitable for the production of abundant fusion reactions. The process is analyzed by a Fokker-Planck equation with a Kennel-Engelmann quasilinear-type rf diffusion term, and an explicit analytic solution is found for the one-dimensional case. Using the resonant-ion distribution function thus derived, and the Duane-formula fit to the D-T fusion cross-section, the computed efficiencies for the rf two-component formation process in a $Z = 1$ plasma show $Q_{RF} \equiv$ (nuclear power out)/(rf power in) values significantly above unity.

ACKNOWLEDGMENTS

REFERENCES

[1] DAWSON, J. M., FURTH, H. P., and TENNEY, F. H., Phys. Rev. Letters 26 (1971) 1156.

[2] STIX, T. H., Phys. Fluids 1 (1958) 308.

[3] YOSHIKAWA, S., ROTHMAN, M. A., and SINCLAIR, R. M., Phys. Rev. Letters 14 (1965) 214.

[4] ADAM, J., and SAMAIN, A., Fontenay-aux-Roses, Report EUR-CEA-FC-579 (1971) 29.

[5] PERKINS, F. W., Symposium on Plasma Heating and Injection, Varenna (1972) 20.

[6] JASSBY, D. L., 2nd Conference on RF Heating, Lubbock, Texas, (1974).

[7] HOOKE, W. M., ROTHMAN, M. A., AVIVI, P., ADAM, J., Phys. Fluids 5 (1962) 864.

[8] CHUNG, K., and ROTHMAN, M. A., Phys. Fluids 10 (1967) 2634.

[9] ADAM, J., CHANCE, M., EUBANK, H., GETTY, W., HINNOV, E., HOOKE, W. M., HOSEA, J., JOBES, F., PERKINS, F., SINCLAIR, R., SPERLING, J., and TAKAHASHI, H., IAEA-CN-33/A3-2 (1974).

[10] STIX, T. H., The Theory of Plasma Waves, McGraw-Hill, New York (1962), Eq. (5-26).

[11] BERNSTEIN, I. B., and TREHAN, S. K., Nuclear Fusion 1 (1960) 3, Eq. (24).

[12] CHANCE, M., and PERKINS, F. W., private communication. See also Ref. [9], Figure 6.

[13] STIX, T. H., (1962), op. cit., Eq. (8-10).

[14] ADAM, J., and SAMAIN, A., op. cit. An incorrect expression is used for the circumference of a circle in Eq. (2), p. 32, and the value cited there for $\bar{P}$ is too large by a factor of 2.

[15] KENNEL, C. F., and ENGELMANN, F., Phys. Fluids $\underline{9}$ (1966) 2377.

[16] SPITZER, L., Jr., The Physics of Fully Ionized Gases, 2nd Revised Edition, Interscience, New York (1962).

[17] COHEN, R. S., SPITZER, L., Jr., and ROUTLY, P. M., Phys. Rev. $\underline{80}$ (1950) 230.

[18] DUANE, B. H., Battelle Pacific Northwest Laboratories, BNWL-1685 (1972) 75.
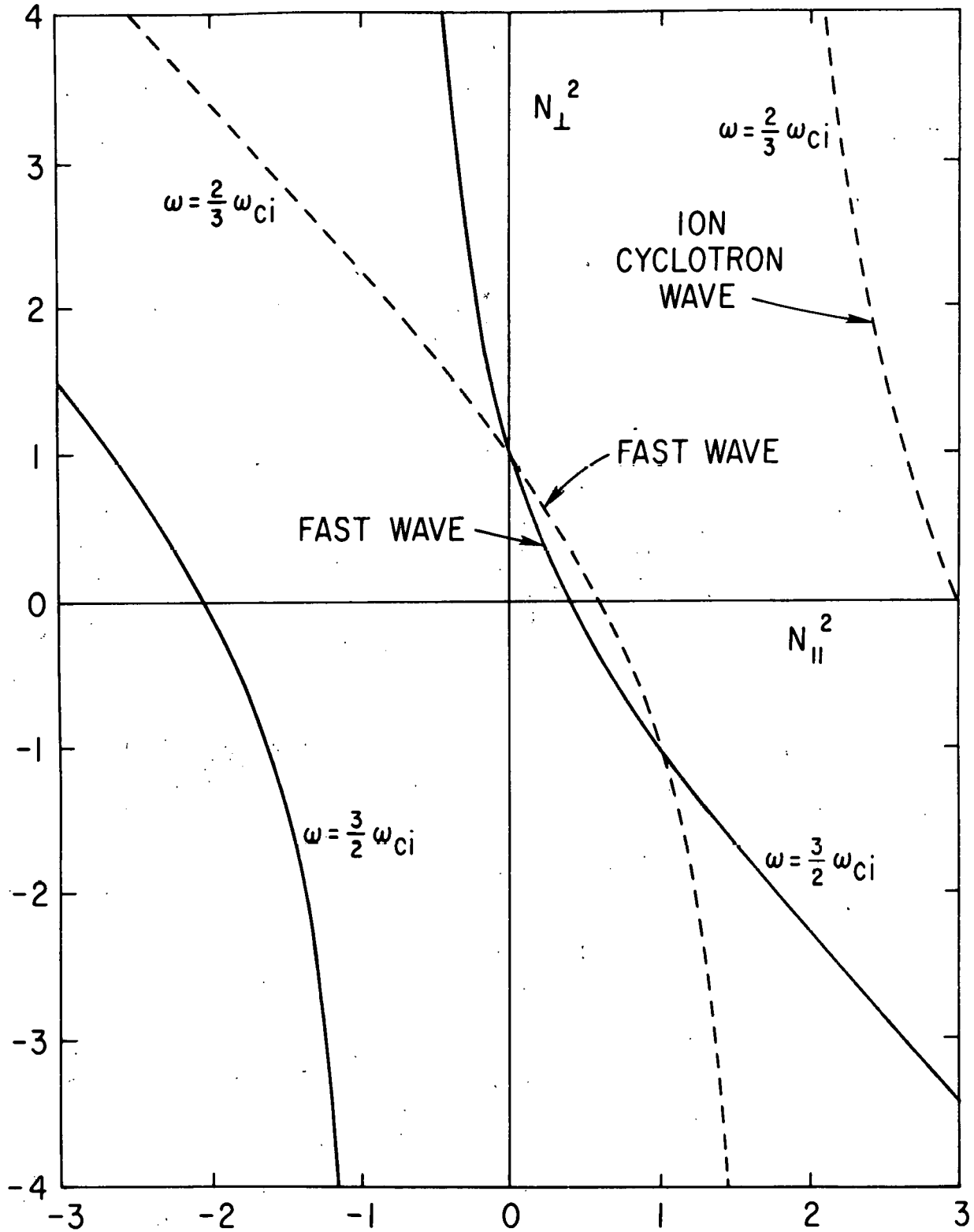
753034

Fig. 1. Dispersion curves for hydromagnetic waves above and below the ion cyclotron frequency. $N_{\parallel}$ and $N_{\perp}$ are the Alfvén refractive indices.
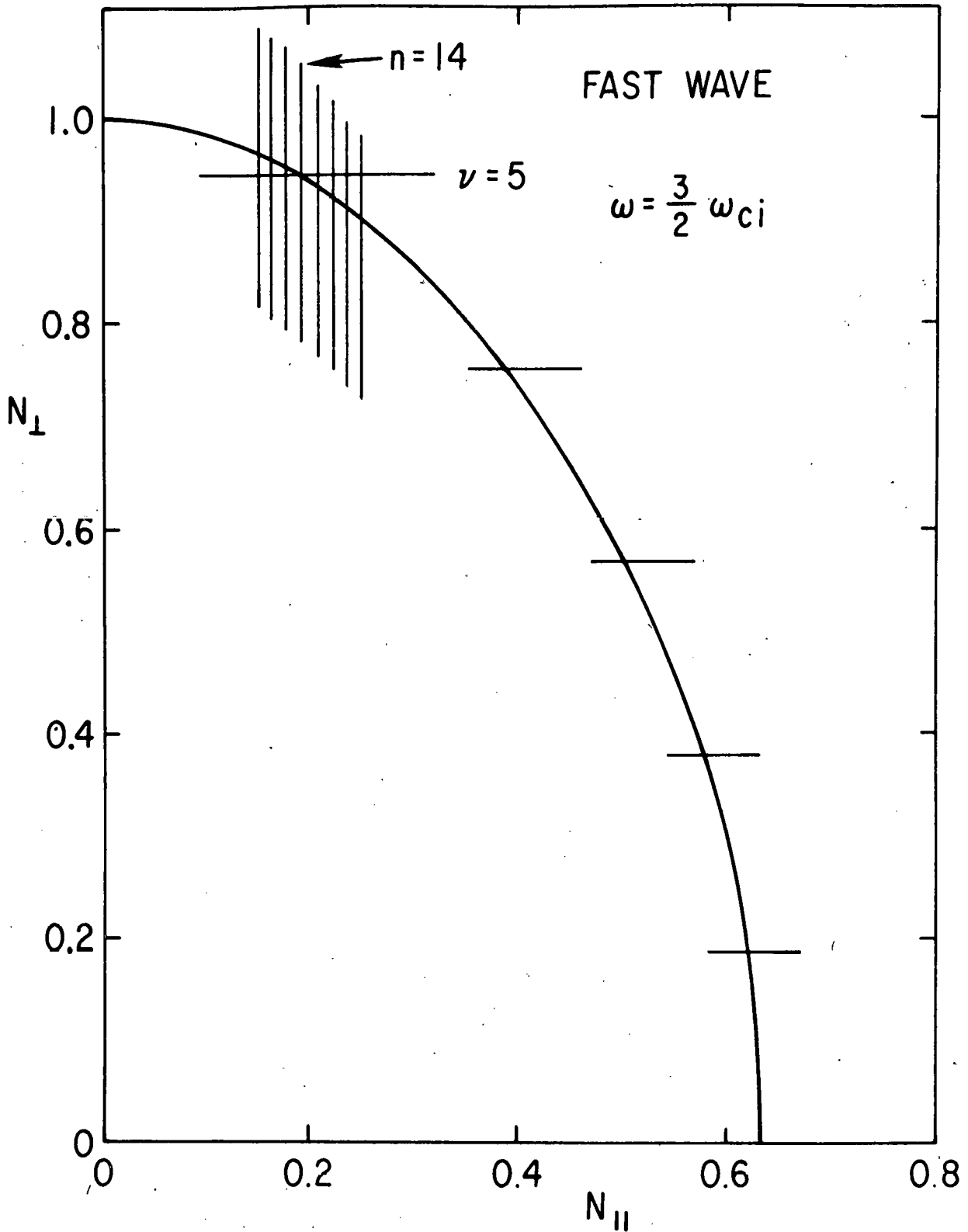
Fig. 2. Dispersion curve for the hydromagnetic fast wave at $\omega = 1.5 \, \omega_{ci}$. The curve here retraces the solid curve through just the first quadrant of Fig. 1. The grid lines correspond to the different poloidal and toroidal mode numbers. Actually, each poloidal (ν) mode is a ($2\nu - 1$)-fold multiplet, and each toroidal (n) mode is a doublet.
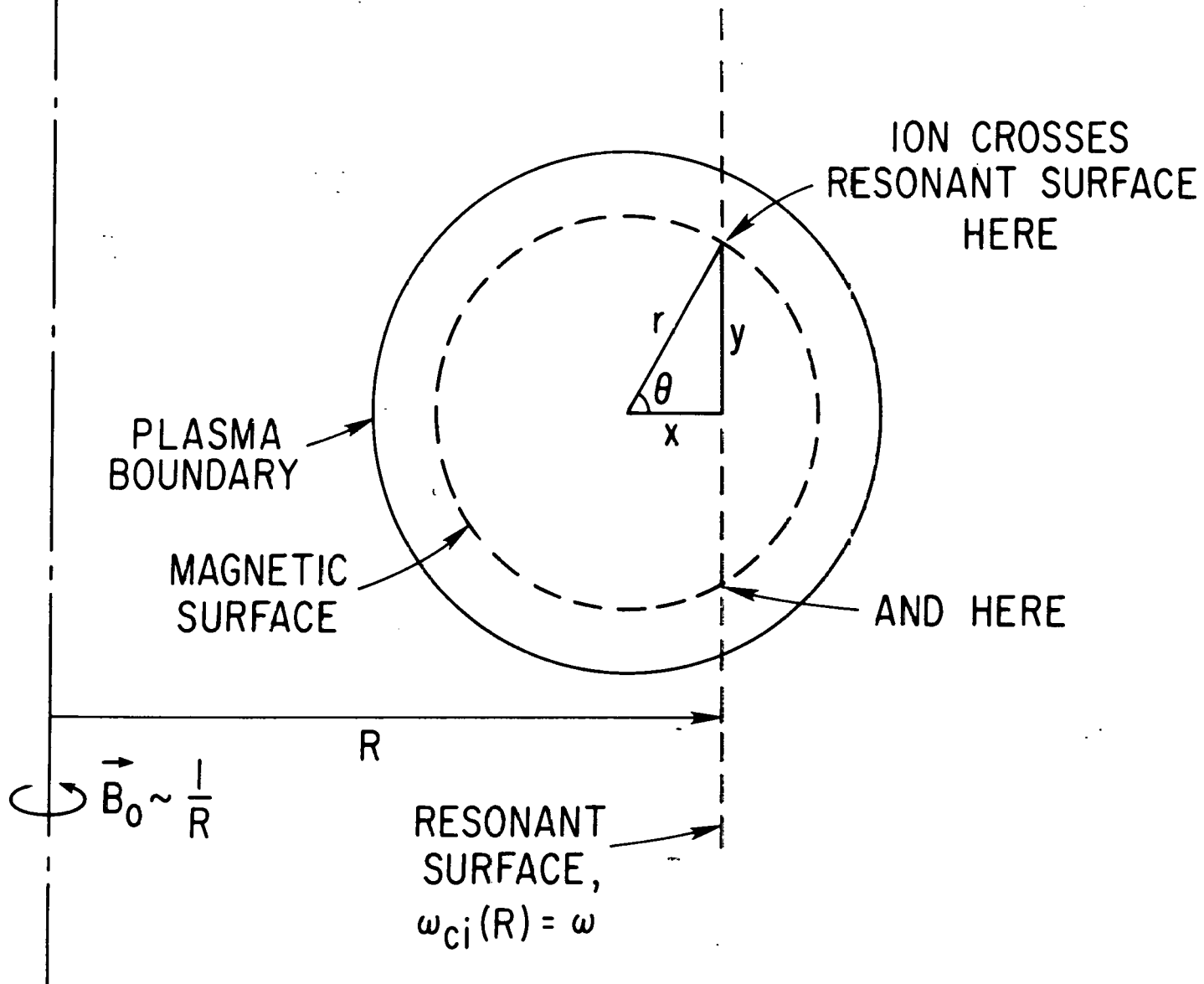
753033

Fig. 3. Geometry for cyclotron resonance excitation in a
torus. Due to the 1/R dependence of B, the resonance region is
a vertical cylindrical shell. Ions moving along a magnetic line of
force and confined to a magnetic surface will intersect the resonance
shell above and below the midplane.
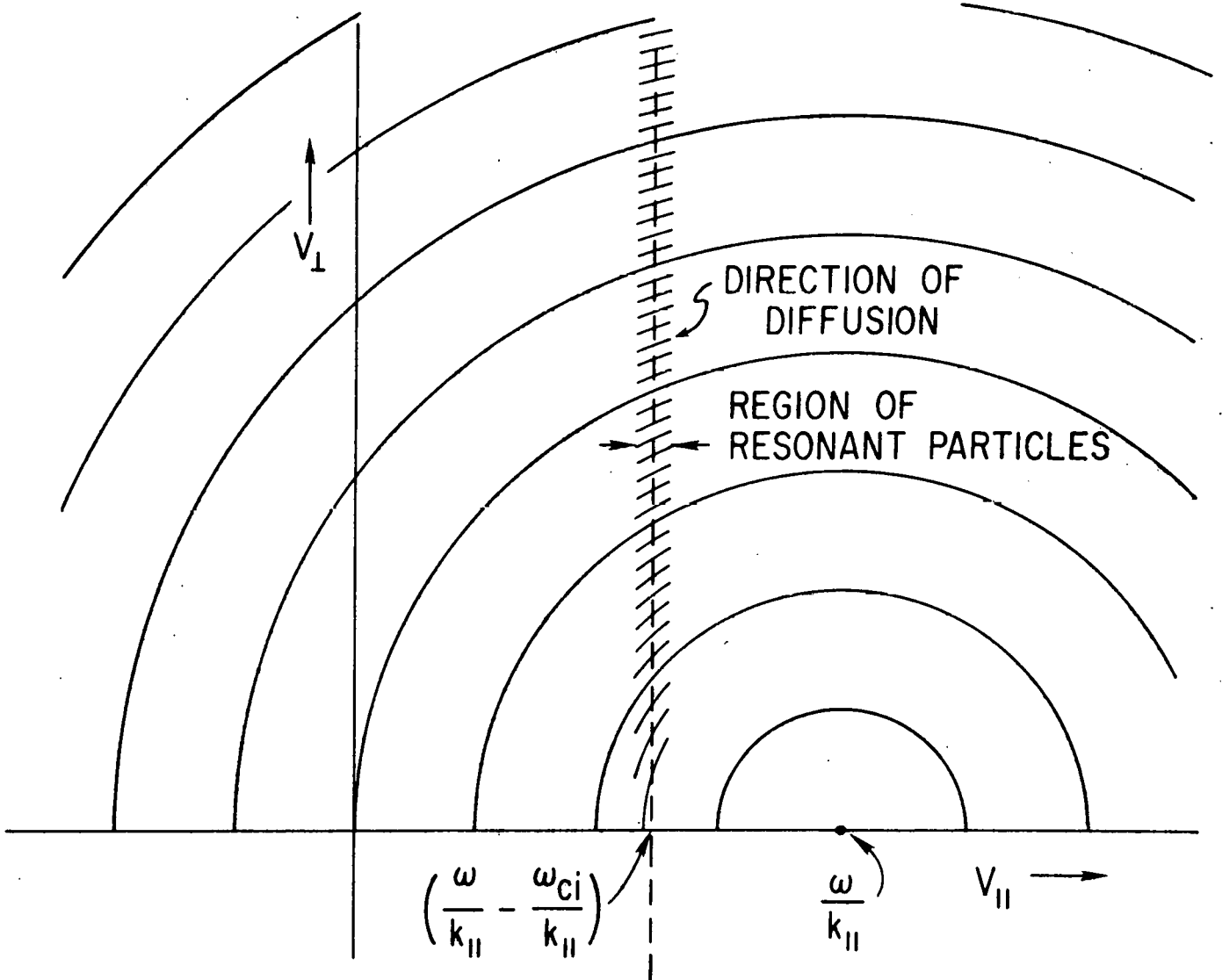
Fig. 4. Contours for quasilinear diffusion. The quasilinear diffusion operator is a gradient operator in velocity space along the indicated circles. Diffusion takes place just in the circumferential direction, but only where the resonance condition is satisfied, i.e., only where the circles intersect the vertical lines.
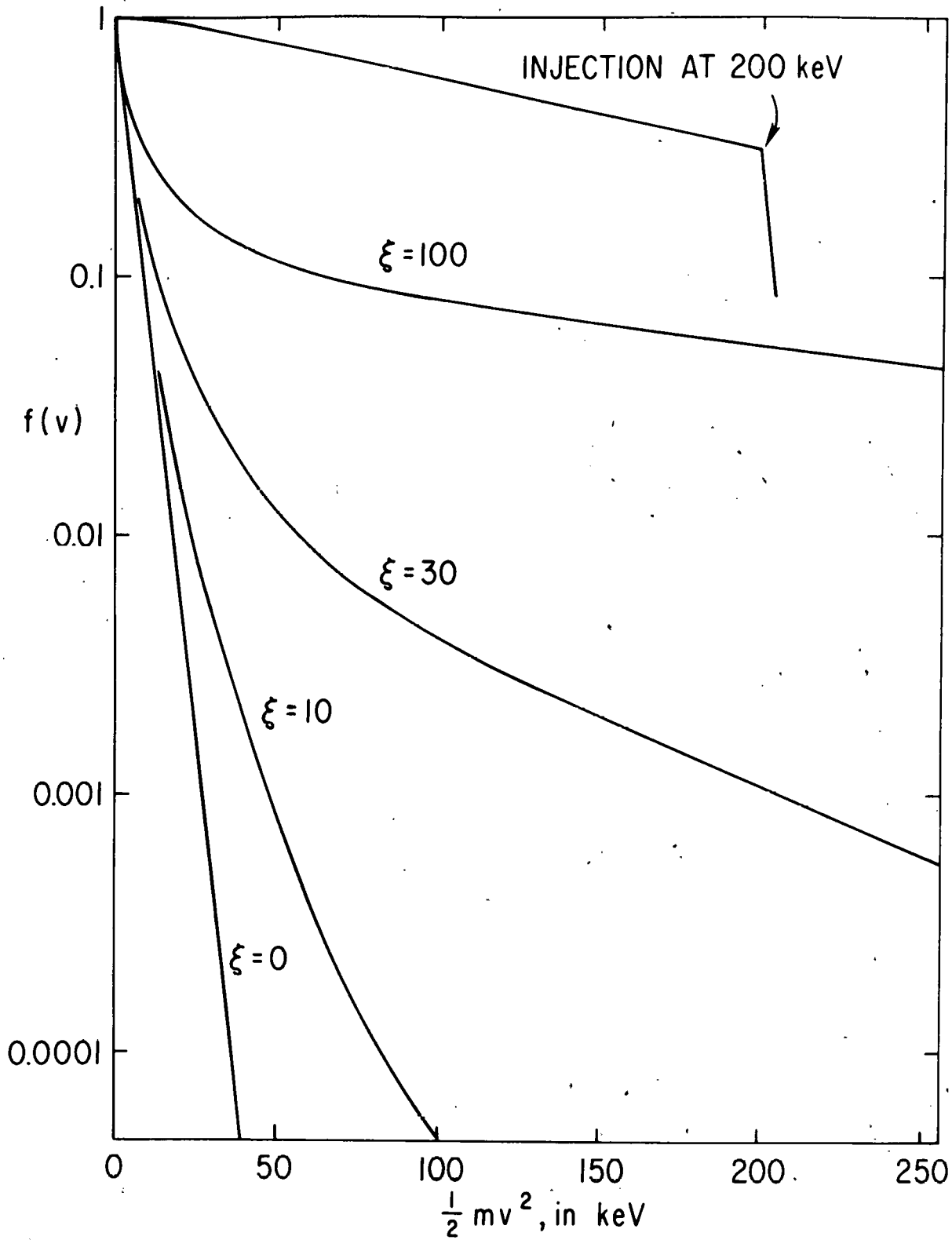
Fig. 5. Plots of f(v) versus E for the plasma parameters of the example in Section 7, and for different levels (ξ) of rf excitation at the minority-species cyclotron frequency. z_{eff} = 3. The ion velocity distribution for injection at 200 keV into the same plasma is also shown.
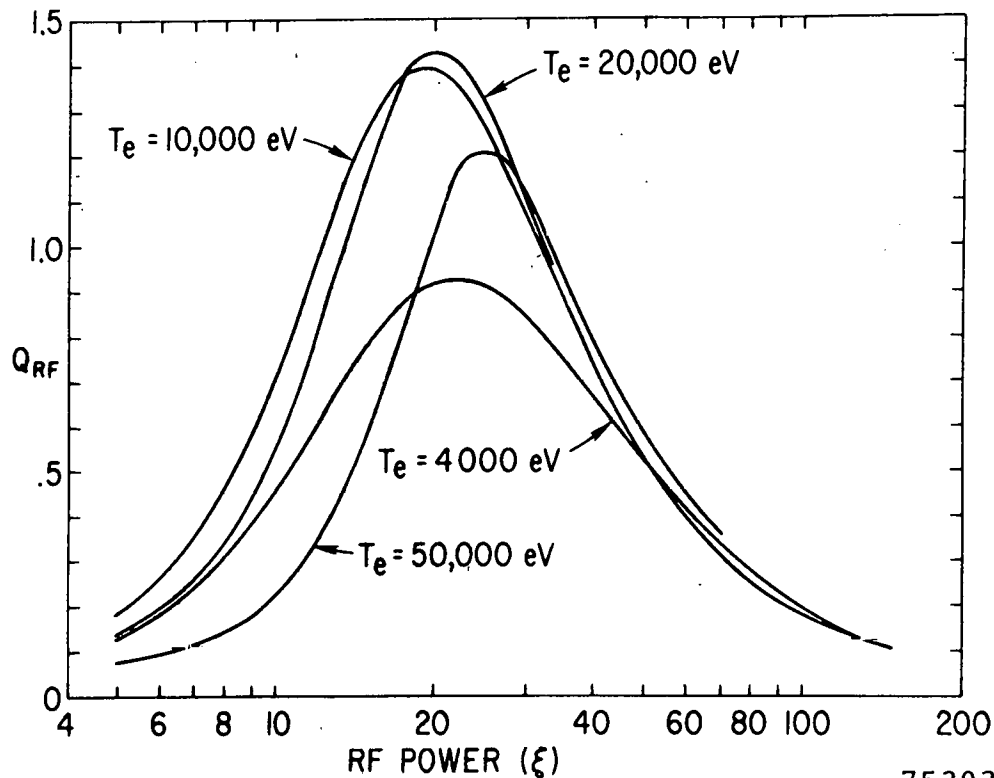
753037

Fig. 6. $Q_{RF} \equiv$ (nuclear power out)/(rf power in is plotted versus rf power per unit volume selectively absorbed by the resonant minority deuterons. $Z_{eff} = 1$.

753036

Fig. 7. Q_{RF} versus rf power for kT_e = keV, for Z_{eff} = 1 and 3, and for temperatures of 1 keV and 4 keV for the background triton ions.